Article

Single-Laser-Shot-Induced Complete Bidirectional Spin Transition at Room Temperature in Single Crystals of (Fe (pyrazine)(Pt(CN)))

Saioa Cobo, Denis Ostrovskii, Se#bastien Bonhommeau, Laure Vendier, Ga#bor Molna#r, Lionel Salmon, Koichiro Tanaka, and Azzedine Bousseksou

J. Am. Chem. Soc., **2008**, 130 (28), 9019-9024 • DOI: 10.1021/ja800878f • Publication Date (Web): 21 June 2008

J|A|C|S
ARTICLES

Published on Web 06/21/2008

Single-Laser-Shot-Induced Complete Bidirectional Spin Transition at Room Temperature in Single Crystals of (Fe^{II}(pyrazine)($Pt(CN)_4$))

Saioa Cobo,[†] Denis Ostrovskii,[†,‡] Sébastien Bonhommeau,[†] Laure Vendier,[†] Gábor Molnár,[†] Lionel Salmon,[†] Koichiro Tanaka,[‡] and Azzedine Bousseksou*[,†]

Laboratoire de Chimie de Coordination, CNRS UPR-8241, 205 Route de Narbonne, 31077 Toulouse, France, and Department of Physics, Graduate School of Science, Kyoto University, Kyoto 606-8502, Japan

Received February 4, 2008; E-mail: boussek@lcc-toulouse.fr

Abstract: Single crystals of the {Fe^{II}(pyrazine)[$Pt(CN)_4$]} spin crossover complex were synthesized by a slow diffusion method. The crystals exhibit a thermal spin transition around room temperature (298 K), which is accompanied by a 14 K wide hysteresis loop. X-ray single-crystal analysis confirms that this compound crystallizes in the tetragonal *P*4/*mmm* space group in both spin states. Within the thermal hysteresis region a complete bidirectional photoconversion was induced between the two phases (high spin ⇄ low spin) when a short single laser pulse (4 ns, 532 nm) was shined on the sample.

Introduction

The control of the state and the properties of condensed matter by light is an important issue in materials science. Within this broad field much attention has been focused recently on the investigation of photoinduced effects in systems showing cooperative phenomena such as phase transitions. In these systems electron−lattice interactions are considered to play a key role in driving the photoinduced transformation and also to give rise to characteristic photoeffects.[1] Notably, in many cases the observation of a threshold photon density has been reported below which the local excited states do not grow into a new macroscopic domain.[2–10] The macroscopic phase change is observed only when the excitation density exceeds this critical "percolation" value, i.e., when the interactions between the photogenerated species can stabilize the new phase. As this phenomenon is closely related to the concept of critical nucleus size in phase transitions, the notion of photoinduced phase transition (PIPT) was introduced.[1] The lattice relaxation which follows the (local) optical excitation may also lead to a "cascade" phenomenon and thus to very high photoconversion efficiencies. For example, in the organic salt $(EDO-TTF)_2PF_6$ a transition from the insulator phase to the metal phase can be induced by ultrashort (femtosecond) light pulses. In this system the reported conversion efficiency reaches 500 molecules for a single photon, and the threshold photon density for the onset of the phenomenon corresponds to one photon for every 1500 EDO−TTF molecules.[8]

In this context, iron(II) spin crossover (SCO) complexes constitute an attractive research target for studying photoinduced phenomena as their spin state can be reversibly modified by light irradiation. Moreover, in many cases, strong, long-range elastic interactions arise between the metal centers leading to first-order thermal phase transition and hysteresis phenomena.[11] Inside the hysteresis loop the macroscopic potential barrier is sufficiently high to make the lifetime of the metastable phases virtually infinite. Therefore, if one succeeds in generating by light a macroscopic domain of the new phase, this latter will be stable toward thermal fluctuations. However, as the lifetime of the local excited spin states is very short at high temperatures (typically in the microsecond to nanosecond range at 295 K) only a short and intense light pulse can generate a sufficiently high excitation density. Recently, a few experimental results have been published describing the effects of short laser pulses on SCO complexes within the thermal hysteresis region.[12–14]

[†] CNRS UPR-8241.
[‡] Kyoto University.

(1) Nasu, K., Ed. *Photoinduced Phase Transitions*; World Scientific Publishing: Singapore, 2004.
(2) Koshihara, S.; Tokura, Y.; Takeda, K.; Koda, T. *Phys. Rev. Lett.* **1992**, *68*, 1148.
(3) Koshihara, S.; Tokura, Y.; Takeda, K.; Koda, T. *Phys. Rev. B* **1995**, *52*, 6265.
(4) Koshihara, S.; Takahashi, I.; Sakai, H.; Tokura, Y.; Luty, T. *J. Phys. Chem. B* **1999**, *103*, 2592.
(5) Hosaka, N.; Tachibana, H.; Shiga, N.; Matsumoto, M.; Tokura, Y. *Phys. Rev. Lett.* **1999**, *82*, 1672.
(6) Matsuzaki, H.; Matsuoka, T.; Kishida, H.; Takizawa, K.; Miyasaka, H.; Sugiura, K.; Yamashita, M.; Okamoto, H. *Phys. Rev. Lett.* **2003**, *90*, 046401.
(7) Collet, E.; Lemée-Cailleau, M.-H.; Buron-Le Cointe, M.; Cailleau, H.; Wulff, M.; Luty, T.; Koshihara, S.-Y.; Meyer, M.; Toupet, L.; Rabiller, P.; Techert, S. *Science* **2003**, *300*, 612.
(8) Chollet, M.; Guerin, L.; Uchida, N.; Fukaya, S.; Shimoda, H.; Ishikawa, T.; Matsuda, K.; Hasegawa, T.; Ota, A.; Yamochi, H.; Saito, G.; Tazaki, R.; Adachi, S.; Koshihara, S. *Science* **2005**, *307*, 86.
(9) Liu, H. W.; Matsuda, K.; Gu, Z. Z.; Takahashi, K.; Cui, A. L.; Nakajima, R.; Fujishima, A.; Sato, O. *Phys. Rev. Lett.* **2003**, *90*, 167403.
(10) Liu, H.; Fujishima, A.; Sato, O. *Appl. Phys. Lett.* **2005**, *86*, 122511.
(11) Gütlich, P.; Goodwin, H. A. *Top. Curr. Chem.* **2004**, *233*, 12.
(12) Freysz, E.; Montant, S.; Létard, S.; Létard, J.-F. *Chem. Phys. Lett.* **2004**, *394*, 318.
(13) Liu, H.; Fujishima, A.; Sato, O. *Appl. Phys. Lett.* **2005**, *86*, 122511.
(14) Bonhommeau, S.; Molnár, G.; Galet, A.; Zwick, A.; Real, J.-A.; McGarvey, J. J.; Bousseksou, A. *Angew. Chem., Int. Ed.* **2005**, *44*, 4069.

The first light-induced low-spin to high-spin (LS → HS) transition in the hysteresis region of an SCO complex was achieved by applying a 8 ns laser pulse at around 170 K on the compound $[Fe(PM\text{-}BiA)_2(NCS)_2]$ (PM-BIA = *N*-2′-pyridylmethylene-4-aminobiphenyl).[12,15] These authors evidenced a partial LS to HS conversion using a single laser pulse of 14 mJ/cm^2 (at 532 nm). Further laser pulses had no effect on the final state and the reversible (HS to LS) conversion was not achieved either. Time-resolved optical reflectivity measurements revealed that the photoexcitation converted first the whole irradiated volume to the pure HS form (transient state) and the final HS + LS mixture state was reached by the system only after a relatively slow (a few seconds) relaxation.[12,15] This finding indicates also that the main driving force of the process is not laser-induced heating. Somewhat later Liu et al.[10] reported similar results on the compound $FeL(CN)_2 \cdot H_2O$ (where L is a Schiff-base macrocyclic ligand) at 216 K. These authors observed thresholds in LS to HS photoconversion for both excitation density and photon energy. The correlation of the spectral dependence of the conversion efficiency and the optical absorption spectra provided convincing evidence that laser-heating process was not relevant in this phenomenon.[10] More recently, we have reported on single-laser-pulse-induced reversible spin-state switching phenomena at room temperature in the compound $\{Fe(pyrazine)[Pt(CN)_4]\}$ (**1**).[14] However, the polycrystalline nature of the investigated sample made difficult any quantitative analysis and raised questions whether the apparently very incomplete HS to LS transition, which has not been observed in other SCO complexes,[12,13] is a genuine photoinduced effect.

The three-dimensional coordination network **1** has been reported for the first time by Niel et al.[16] It undergoes a cooperative spin-state change with a reproducible, large thermal hysteresis loop around room temperature in its dehydrated form, but the application of external pressure or light irradiation allows also the manipulation of its spin state.[14,17] In addition to these properties, the possibility to assemble these systems as thin films[18] or even the fabrication of nanostructures[19] has been also shown recently. A further development of these studies would be highly promoted by the growth of single crystals for a quantitative investigation of light-induced effects and to extend the knowledge on the relationship between structural features and the physical properties.

In this paper, we describe a method for the synthesis of single crystals of **1**. The SCO in these crystals have been evidenced by crystallographic and magnetic measurements as well as by Raman spectroscopy. With the use of these crystals, we succeeded to observe, for the first time, a complete and bidirectional photoconversion between the pure LS and HS forms induced by a single laser shot.

Results and Discussion

Yellow needle crystals of **1** have been synthesized by diffusion in liquid/liquid phase. Upon cooling the crystal's color turns to red indicating the occurrence of SCO. The obtained crystals were sufficiently large for optical measurements, but they were only weakly diffracting limiting thus the scope of the X-ray crystallographic analysis mostly to the lattice parameters (Table 1). As expected, the crystal packing is similar to what was evaluated from powder X-ray analysis of the hydrated compound (Figure 1).[11] The complex presents the tetragonal space group *P*4/*mmm* in the 293−120 K temperature range, regardless of the spin state of Fe^{II}. Upon lowering the temperature to 223 K a remarkable decrease has been observed in the lattice parameters during the HS to LS transition. This unit cell contraction is anisotropic: 3.22% and 7.06% for the *a*(*b*)- and *c*-axes, respectively, and the volume of the unit cell is reduced by ca. 13% (52 Å^3), attesting the high flexibility of the crystal (Figure 2). This relative volume change is very large when compared to the generally observed 1−6% variation in SCO complexes with FeN_6 coordination polyhedra,[20] which can be explained by the rather small unit cell volume of the complex **1**. Another remarkable feature of the crystal lattice is the slightly negative thermal expansion in the LS phase (V_{120K} = 349.16(10)

Table 1. Crystal Structure Analysis of $\{Fe(pyrazine)[Pt(CN)_4]\}$

	T = 293 K	T = 223 K
chem formula	$C_8H_4N_6Fe_1Pt_1$	$C_8H_4N_6Fe_1Pt_1$
Fw	435.10	435.10
a, Å	7.4314(6)	7.1710(6)
b, Å	7.4314(6)	7.1710(6)
c, Å	7.2468(18)	6.7700(18)
β deg	90	90
V, Å^3	400.21(11)	348.14(10)
Z	1	1
space group	*P*4/*mmm*	*P*4/*mmm*
λ, Å	0.71073	0.71073
ρ_{calc}, g·cm^{-3}	1.789	2.056
μ, cm^{-1}	0.9620	1.1059
$R[I > 2\sigma(I)]^a$	0.0708	0.0644
$wR^2[I > 2\sigma(I)]^b$	0.1695	0.1536

^{a} $R = \sum(|F_o| - |F_c|)/\sum|F_o|$. ^{b} $wR^2 = \{\sum[w(F_o^2 - F_c^2)^2]/\sum[w(F_o^2)^2]\}^{1/2}$.

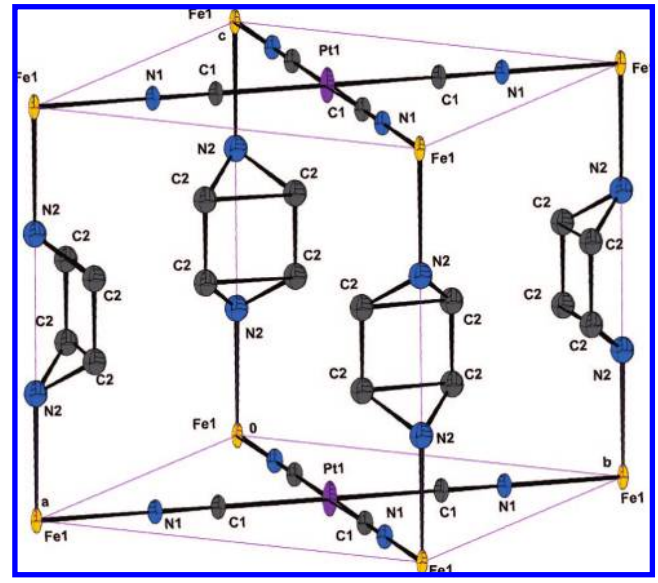

Figure 1. Cameron view (ellipsoid at 30% probability level) of the disordered $\{Fe(pyrazine)[Pt(CN)_4]\}$ complex at 293 K with atom numbering scheme.

(15) Degert, J.; Lascoux, N.; Montant, S.; Létard, S.; Freysz, E.; Chastanet, G.; Létard, J.-F. *Chem. Phys. Lett.* **2005**, *415*, 206.
(16) Niel, V.; Martínez-Agudo, J. M.; Muñoz, M. C.; Gaspar, A. B.; Real, J.-A. *Inorg. Chem.* **2001**, *40*, 3838.
(17) Molnar, G.; Niel, V.; Real, J. A.; Dubrovinsky, L.; Bousseksou, A.; Mc-Garvey, J. J. *J. Phys. Chem. B* **2003**, *107*, 3149.
(18) Cobo, S.; Molnár, G.; Real, J. A.; Bousseksou, A. *Angew. Chem., Int. Ed.* **2006**, *45*, 5786.
(19) Molnár, G.; Cobo, S.; Real, J.-A.; Carcenac, F.; Daran, E.; Vieu, C.; Bousseksou, A. *Adv. Mater.* **2007**, *19*, 2163.
(20) Guionneau, P.; Marchivie, M.; Bravic, G.; Letard, J. F.; Chasseau, D. *Top. Curr. Chem.* **2004**, *234*, 97.

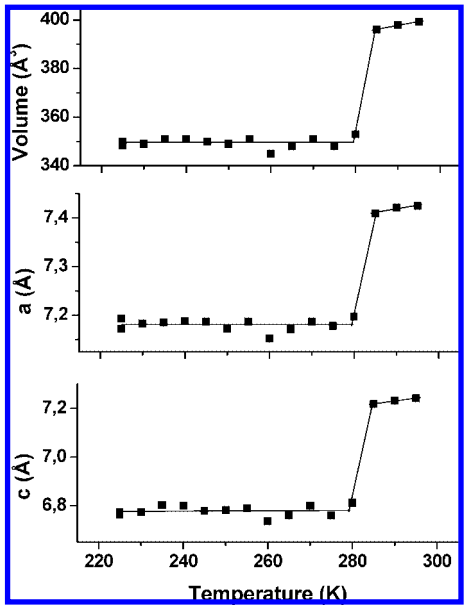

Figure 2. Thermal variation of the unit cell parameters of {Fe(pyrazine)[Pt(CN)$_4$]} in the cooling mode. (Lines are inserted to guide the eye.)

Å^3, V_{225K} = 348.41(7) Å^3), but the discussion of this singular phenomenon is out of the scope of the present paper.

Figure 3 shows the $\chi_M T$ versus T plot, where χ_M stands for the molar magnetic susceptibility of the crystals of **1**. The $\chi_M T$ value in the high-temperature region is about 3.5 cm^3 K mol^{-1} that corresponds to the HS ($S = 2$) state of the Fe^{II} ions. Upon cooling the sample, the value of $\chi_M T$ remains constant down to 295 K. Below this temperature it undergoes a sharp decrease characteristic of a first-order phase transition and drops to 0.1 cm^3 K mol^{-1} at ca. 280 K, indicating that the SCO is virtually complete. The warming mode reveals the occurrence of a 14 K wide thermal hysteresis loop, with transition temperatures for the cooling ($T_{1/2}^{down}$) and warming ($T_{1/2}^{up}$) modes equal to 291 and 305 K, respectively. The magnetic properties of the powder form of **1** have been reported earlier, and a similar though larger (24 K) hysteresis loop was observed.[14]

Raman spectra of single crystals of **1** were also found very similar to those reported for polycrystalline powders[21] and thin films[18] (Figure 4 and Supporting Information Figure S1). Typical spectra exhibit strong peaks of CN stretching vibrations around 2200 cm^{-1} and internal modes of pyrazine in the region between 600 and 1600 cm^{-1}. Below 600 cm^{-1}, several spectral bands characteristic for metal−ligand vibrations and lattice phonons can be observed. In the case of crystals several Raman modes clearly demonstrate high degree of polarization that has obviously not been observed in powder samples. When SCO occurs, the Raman spectra undergo characteristic changes (Figure 4). For example, an in-plane bending mode of the pyrazine ring shifts from 675 to 645 cm^{-1} when going from the LS to the HS state. In a more quantitative way, the plot of temperature dependence of the intensity ratio of two Raman modes at 1032 and 1232 cm^{-1} is incorporated in Figure 3 matching closely the hysteresis observed in the magnetic measurements.

To investigate the effect of a short laser pulse on the spin state of a single crystal, we have recorded Raman spectra before and after the photoexcitation. The insets of Figure 3 show Raman spectra recorded in the spectral region of interest before and after irradiation by a single pulse of green light (532 nm, 4 ns). These spectra were recorded within the hysteresis loop at 299 K in the heating cycle (point A) and at 294 K in the cooling cycle (point C). The shift of the Raman frequency from 675 to 645 cm^{-1} and vice versa proves clearly that the spin state of iron(II) ions in single crystals of **1** is changed by the laser shot. These photoinduced spin transitions are also confirmed by a variation of the intensity ratio of the 1032 and 1232 cm^{-1} modes from 0.22 to 3.41 (A → B) and from 3.33 to 0.25 (C → D), which corresponds to a virtually complete LS ↔ HS conversion. In all cases the photoinduced transition manifested itself as a significant color change of the crystals (Supporting Information Figures S2 and S3). We should stress also that the geometry of the experiment—pulsed irradiation of the crystal from the bottom and excitation of Raman scattering from the top (Figure 5 and Supporting Information Figure S4)—ensures that the observed full conversion of the spin state has happened through the whole crystal volume. The fact that the high-temperature (HS) phase can be fully converted to the low-temperature (LS) phase proves that the thermal effects of the laser pulse are negligible in the given experimental conditions.

Significant difference, however, was observed in the pulse energy needed to achieve different types of spin transition. In the LS → HS case (A → B) complete conversion has been obtained when the pulse energy reached a value of about 20 mJ/cm^2. At the same time, complete HS → LS transition (C → D) was repeatedly observed only at comparatively low energies (∼5 mJ/cm^2 per pulse) and disappeared with further power increase. The origin of this energy dependence is not completely clear so far, and more detailed investigation of the conversion rate dependence on pulse energy, temperature, and other parameters is needed, but this type of measurements are only feasible on thin film samples (<1 μm) due to the high optical density of the compound at the exciting wavelength.

From a theoretical point of view one should consider that within the hysteresis loop there exists a threshold for the photoinduced as well as thermally induced spin transition due to the energy barrier which separates the two phases. An explanation about the dependence in photoexcitation energy density can be proposed using the mean-field model of Slichter and Drickamer,[22] formally identical to a mean-field Ising-like model.[23] Within this approach, the free energy (G) of a system in which thermal evolution of the HS fraction (γ_{HS}) exhibits a hysteresis loop is described by the equation

$$G = \gamma_{HS}\Delta H + \Gamma\gamma_{HS}(1-\gamma_{HS}) + T[R(\gamma_{HS}\ln\gamma_{HS} + (1-\gamma_{HS})\ln(1-\gamma_{HS})) - \gamma_{HS}\Delta S] \quad (1)$$

and the hysteresis loop can be simply simulated (Supporting Information Figure S5) by resolving the self-consistent equation leading to the steady states of the aforementioned system:

$$\ln\left(\frac{1-\gamma_{HS}}{\gamma_{HS}}\right) = \frac{\Delta H + \Gamma(1-2\gamma_{HS})}{RT} - \frac{\Delta S}{R} \quad (2)$$

where R is the gas constant, Γ is a phenomenological interaction parameter, ΔH ($= H_{HS} - H_{LS}$) is the transition enthalpy, and ΔS ($= S_{HS} - S_{LS}$) is the transition entropy. It should be noted that such a simple mean-field model is useful to understand the different experimental observations, but it cannot be expected

(21) Molnár, G.; Niel, V.; Gaspar, A. B.; Real, J.-A.; Zwick, A.; Bousseksou, A.; McGarvey, J. J. *J. Phys. Chem. B* **2002**, *106*, 9701.
(22) Slichter, C.; Drickamer, H. *J. Chem. Phys.* **1972**, *56*, 2142.
(23) Bousseksou, A.; Nasser, J.; Linares, J.; Boukheddaden, K.; Varret, F. *J. Phys. I* **1992**, *2*, 1381.

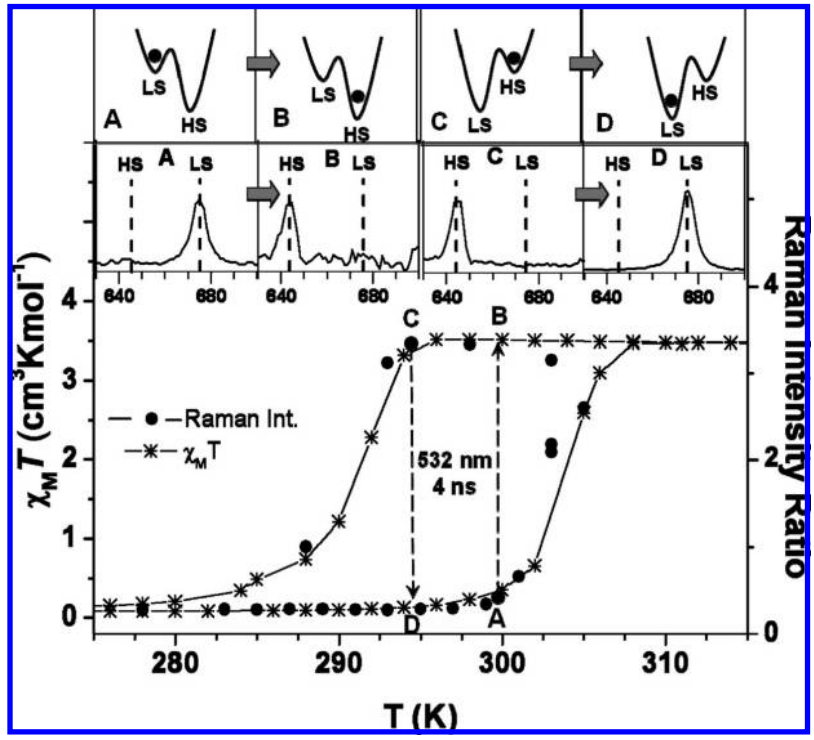

Figure 3. Temperature dependence of the $\chi_M T$ product and the intensity ratio of two Raman modes at 1032 and 1232 cm^{-1} (I_{1032}/I_{1232}) for {Fe(pyrazine)[Pt(CN)$_4$]} single crystals upon cooling and heating. (Lines are inserted to guide the eye.) The insets A−D show the schematic free energy diagrams at the corresponding points of the hysteresis loop and typical Raman spectra before (A and C) and after (B and D) single-pulse irradiation of a crystal (532 nm, 4 ns). Dashed lines mark the frequencies of HS and LS modes at 645 and 675 cm^{-1}, respectively.

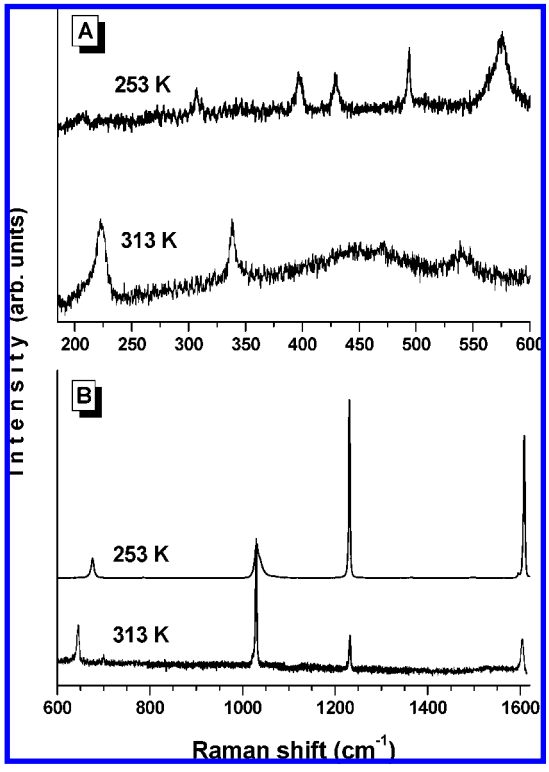

Figure 4. Raman spectra of {Fe(pyrazine)[Pt(CN)$_4$]} crystals in the low-frequency (A) and high-frequency (B) regions.

to reproduce quantitatively the photoinduced effects for various reasons. Notably, the material is regarded homogeneous in the frame of our theoretical approach, whereas PIPT should involve both nucleation and growth of many domains.[24–29]

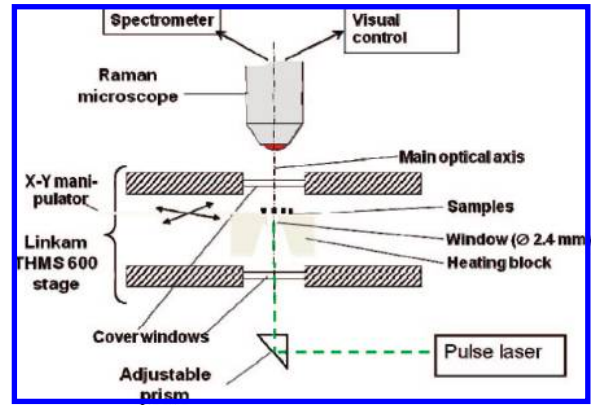

Figure 5. Schematic drawing of the experimental setup for pulsed laser experiments. The Raman spectra of the sample were acquired from the upper crystal face, opposite to that subjected to the pulsed irradiation through a tapered hole in the cooling block of the Linkam cryostage.

Figure 6displays the free energy of the system as a function of γ_{HS} in the temperature range of the hysteresis loop. The curves have been calculated using eq 1 with the parameters $\Delta H = 25.35$ kJ mol^{-1}, $\Delta S = 85$ J K^{-1} mol^{-1}in agreement with the

(24) Collet, E.; Buron-Le Cointe, M.; Cailleau, H. *J. Phys. Soc. Jpn.* **2006**, *75*, 011002.
(25) Ogawa, Y.; Koshihara, S.; Koshino, K.; Ogawa, T.; Urano, C.; Takagi, H. *Phys. Rev. Lett.* **2000**, *84*, 3181.
(26) Molnár, G.; Bousseksou, A.; Zwick, A.; McGarvey, J. *Chem. Phys. Lett.* **2003**, *367*, 593.
(27) Pillet, S.; Hubsch, J.; Lecomte, C. *Eur. Phys. J. B* **2004**, *38*, 541; **2006**, *49*, 265.
(28) Moritomo, Y.; Kamiya, M.; Nakamura, A.; Nakamoto, A.; Kojima, N. *Phys. Rev. B* **2006**, *73*, 012103.
(29) Ichiyanagi, K.; Hebert, J.; Toupet, L.; Cailleau, H.; Guionneau, P.; Létard, J. F.; Collet, E. *Phys. Rev. B* **2006**, *73*, 060408.

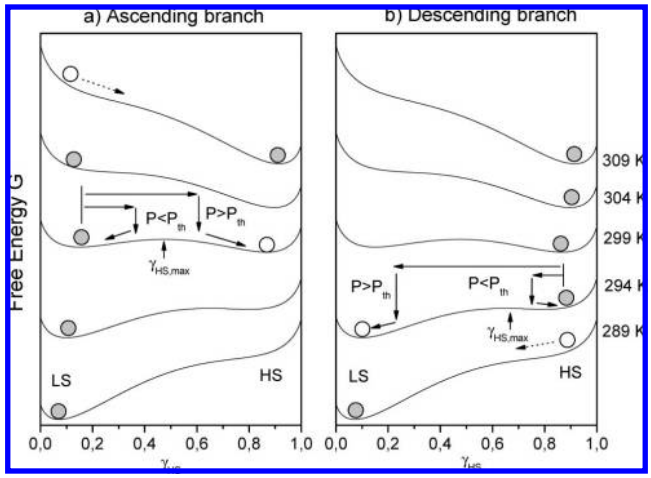

Figure 6. Free energy of the {Fe(pyrazine)[Pt(CN)$_4$]} complex as a function of the HS fraction at different temperatures within the hysteresis region calculated using eq 1. Parameter values are $\Delta H = 25.35$ kJ mol^{-1}, $\Delta S = 85$ J K^{-1} mol^{-1}, and $\Gamma = 6.25$ kJ mol^{-1}. The threshold effect observed on the ascending (a) and descending (b) branches of the hysteresis loop of {Fe(pyrazine)[Pt(CN)$_4$]} is depicted schematically. Gray spheres indicate the thermal population, and white spheres indicate the photoinduced population with one laser shot at 532 nm.

literature,[30] and $\Gamma = 6.25$ kJ mol^{-1} resulting from the simulation of the hysteresis loop (Supporting Information Figure S5). The minimum of the potential energy curve increases from $\gamma_{HS} \approx 0$ to $\gamma_{HS} \approx 1$ with temperature. At 299 K in the heating mode, an energy barrier appears around $\gamma_{HS} \approx 0.47$ (noted $\gamma_{HS,max}$). If the system is photoexcited at this temperature in the LS state by a laser pulse (532 nm) an intersystem crossing occurs toward the HS state. When the photoconverted HS fraction is lower than $\gamma_{HS,max}$, the system cannot pass over the macroscopic energy barrier and recovers its initial state. However, if γ_{HS} exceeds $\gamma_{HS,max}$, the irradiated sample reaches a pure HS state. Similarly, when the sample is initially in the HS state ($\gamma_{HS} \approx 1$, Figure 6b), a phase transition occurs if one overcomes $\gamma_{LS,max} = 1 - \gamma_{HS,max} \approx 0.35$ at 294 K and the pure LS state is generated. These $\gamma_{HS,max}$ values correspond hence to a certain photoexcitation energy density threshold (P_{th}). It is important to notice that on the ascending branch of the hysteresis loop this photoinduced transition must be assisted to a certain extent by the laser light induced heating. On the contrary, on the descending branch of the hysteresis loop, heating effects compete with the photoinduced conversion to the stable LS state. This explains why the HS → LS photoconversion efficiency reaches a maximum at about 5 mJ/cm^2 before decreasing. Heat brought by high-energy pulses annihilates thus the optical effect.

Another important feature of the observed phenomena is that a complete photoswitching was obtained at the same photon excitation energy (2.33 eV) in both directions (HS → LS and LS → HS), which can only be explained by the cooperative nature of the system in addition to the overlap of HS and LS absorption bands at this energy. In fact, the optical density of {Fe(pyrazine)[Pt(CN)$_4$]} at this photon energy is rather high in both spin states allowing thus an efficient excitation of the compound in both forms (Figure 7). However, in the absence of cooperative effects photoexcitation of the system would lead to the same final state, according to the branching ratios,

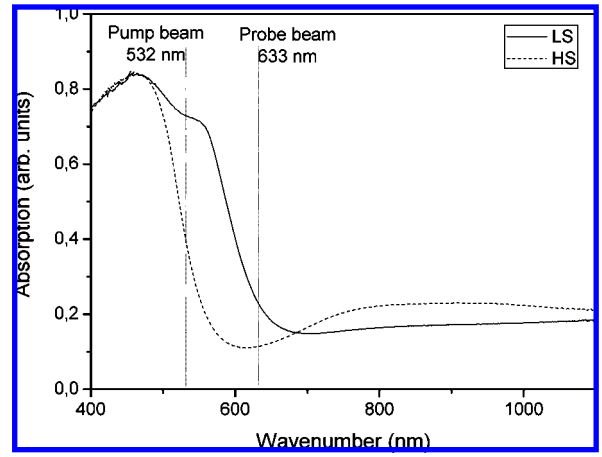

Figure 7. Absorption spectra of polycrystalline {Fe(pyrazine)[Pt(CN)$_4$]} determined by diffuse reflectance measurement in the HS and LS states at 295 K using an integration sphere and a Teflon reference sample. Wavelengths of the pump (532 nm) and probe (633 nm) laser beams are indicated.

independently of the initial state. In the present case the observation of two different final states is thus related to the existence of metastable phases within the hysteresis loop. As depicted in Figure 6, if the exciting light energy density is higher than the "percolation threshold" (P_{th}) the metastable system (either HS or LS) will be converted to the stable state. In this way the cooperative phenomena can stabilize different final states even if the excitation wavelength is the same.

Conclusions

We have synthesized {Fe(pyrazine)[Pt(CN)$_4$]} single crystals and shown that they undergo a HS ⇄ LS thermal spin transition around room temperature with a large hysteresis loop. The crystallographic analysis revealed an unprecedented 13% change of the unit cell volume upon the SCO. Remarkably, in spite of this huge and abrupt volume change the crystals do not break nor change their space group. We have evidenced, for the first time, a complete LS → HS as well as HS → LS photoconversion following a short one-shot laser irradiation of the crystals close to room temperature. This crystal appears thus as an excellent model system for the investigation of the interplay between light excitation and cooperative electron−lattice interactions.

Experimental Section

Synthesis. An 8 mL vial was placed inside a 60 mL jar with stopper. The jar was filled with 0.5 M aqueous solution of pyrazine such that the level of solution was approximately 0.5 cm above the top of the vial. An amount of 2 mL of an aqueous solution of 0.5 M $Fe(BF_4)_2 \cdot 6H_2O$ (cooled on ice) was injected at the bottom of the vial, and 2 mL of a 0.5 M aqueous solution of $K_2Pt(CN)_4 \cdot 3H_2O$ (cooled on ice) was injected at the bottom of the large jar. The jar was closed and then placed in a water bath of 45 °C. After 3 days, a mixture of yellow powder and needle crystals with the size suitable for X-ray analysis were formed. Crystals were isolated and allowed to dry in air for 1 day at room temperature. The dehydration of crystals was performed by heating at 423 K. Anal. Calcd for $C_8H_4N_6Fe_1Pt_1$: C 22.08, H 0.93, N 19.32%. Found: C 23.02, H 0.68, N 19.16%. The observed difference is in agreement with the presence of a small amount of additional pyrazine and water molecules trapped in the pores.

X-ray Analysis. Crystallographic data were collected on a Gemini Oxford Diffraction diffractometer using a graphite-monochromated Mo Kα radiation ($\lambda = 0.71073$ Å). Low-temperature experiments were performed with an Oxford Cryosystems Cryos-

(30) Tayagaki, T.; Galet, A.; Molnár, G.; Muñoz, M.; Zwick, A.; Tanaka, K.; Real, J.; Bousseksou, A. *J. Phys. Chem. B* **2005**, *109*, 14859.

tream cooler device. The final unit cell parameters have been obtained by means of a least-squares refinement. The structures have been solved by direct methods using SIR92[31] and refined by means of least-squares procedures on F^2 with the aid of the program SHELXL97[32] included in the software package WinGX version 1.63.[33] The atomic scattering factors were taken from International Tables for X-Ray Crystallography.[34] All non-hydrogen atoms were anisotropically refined, and in the last cycles of refinement a weighting scheme was used, where weights are calculated from the following formula $w = 1/[\sigma^2(F_o^2) + (aP)^2 + bP]$ where $P = (F_o^2 + 2F_c^2)/3$.

The crystal packing consists of 2D planar metal−cyanide−metal sheets formed of square-planar tetracyanometalate ions connected by six-coordinate Fe^{II} ions. The bidentate pyrazine ligands bridge each 2D layers by the nitrogen atoms through the Fe−N bond to form a 3D network. The pyrazine ligands display positional disorder. The interstitial sites can accommodate water and pyrazine molecules, which were removed almost completely by annealing at 150 °C. We must remark that it was very difficult to find suitable crystals for X-ray analysis. We managed to solve the structure of a small ($0.17 \times 0.06 \times 0.03$ mm^3) and weakly diffracting crystal, but we obtained a low resolution and a small diffraction range ($2\theta < 23.67°$). For this reason, a reliable discussion of bond distances and angles is not possible. One should also note that we found a positive electron density residue of 3.037 e Å^{-3} which could be explained, on the basis of the elementary analysis, by the presence of a small amount of pyrazine molecules trapped in a random manner inside the {Fe(pyrazine)[Pt(CN)$_4$]} porous network.

Physical Measurements. Analysis for C, H, and N were performed after combustion at 850 °C using IR detection and gravimetry by means of a Perkin-Elmer 2400 series II device. Magnetic susceptibility measurements were carried out at heating and cooling rates of 2 K min^{-1} using a Quantum Design MPMS2 SQUID magnetometer operating at 5000 Oe magnetic field. The experimental data were corrected for the diamagnetic contribution. Raman spectra were recorded by means of a LabramHR (Jobin Yvon) Raman spectrometer equipped with an Olympus BXFM microscope (×50 ULWD objective) and a Peltier-cooled CCD detector. With a 600 grooves/mm grating and a slit width of 100 μm the spectral resolution was better than 3 cm^{-1}. Accumulation time was typically 30−100 s. A HeNe laser operating at 632.8 nm was used as an excitation source. The excitation power on the sample was set to 0.07 mW. The sample temperature was controlled using a Linkam THMS600 liquid nitrogen cryostage. At each temperature the sample was allowed to stabilize during 5 min prior to measurements. For pulsed irradiation we used a Continuum Nd:YAG pulsed laser (model Minilite) generating 4 ns long green light pulses ($\lambda = 532$ nm). To investigate light-pulse switching phenomena we recorded the Raman spectra of the sample from the upper crystal face, opposite to that subjected to the pulsed irradiation through a tapered hole in the cooling block (Figure 5 and Supporting Information Figure S4). Prior to pulsed irradiation the sample was cooled (or heated) to the desired temperature at a rate of 1 K min^{-1}, and it was let to stabilize during ca. 30 min. Following the pulsed irradiation Raman spectra were recorded immediately and also 1−2 h later in order to check the stability of the final state.

Acknowledgment. The authors are grateful to S. Seyrac (LCC), L. Rechignat (LCC), and A. van der Lee (University of Montpellier II), for elemental analysis and magnetic and crystallographic measurements. J. A. Real (University of Valencia) is thanked for helpful comments. This work was supported by the ANR project FASTSWITCH and a Grant-in-Aid for Creative Scientific Research.

Supporting Information Available: Experimental details, photos of the crystals, and Raman data. This material is available free of charge via the Internet at http://pubs.acs.org.

JA800878F

(31) Altomare, A.; Cascarano, G.; Giacovazzo, C.; Guagliardi, A. *J. Appl. Crystallogr.* **1993**, *26*, 343–350.
(32) Sheldrick, G. M. *SHELX97 [Includes SHELXS97, SHELXL97, CIFTAB]—Programs for Crystal Structure Analysis*, release 97-2; Institüt für Anorganische Chemie der Universität: Tammanstrasse 4, D-3400 Göttingen, Germany, 1998.
(33) Farrugia, L. *J. Appl. Crystallogr.* **1999**, *32*, 837–838.
(34) *International Tables for X-Ray Crystallography*; Kynoch Press: Birmingham, England, 1974; Vol. IV.